Acta Cryst. (1992). C48, 414–419

Refinement of the Structures of $Sr_3Al_2O_6$ and the Hydrogarnet $Sr_3Al_2(O_4D_4)_3$ by Rietveld Analysis of Neutron Powder Diffraction Data

BY BRYAN C. CHAKOUMAKOS

Solid State Division, Oak Ridge National Laboratory, Oak Ridge, TN 37831-6056, *USA*

GEORGE A. LAGER

Department of Geology, University of Louisville, Louisville, KY 40292, *USA*

AND JAIME A. FERNANDEZ-BACA

Solid State Division, Oak Ridge National Laboratory, Oak Ridge, TN 37831-6393, *USA*

(*Received* 15 *April* 1991; *accepted* 21 *August* 1991)

Abstract. $Sr_3Al_2O_6$, $M_r = 412.81$, cubic, $Pa3$, $a = 15.8556\ (4)$ Å, $V = 3986.0\ (5)$ Å^3, $Z = 24$, $D_x = 4.126$ g cm^{-3}, $\lambda = 1.400$ Å, $\mu R = 0.020$, $T = 295$ K, $R_{exp} = 0.0295$, $R_{wp} = 0.0447$ for 2415 step intensities, $R_{Bragg} = 0.0168$ for 1606 reflections. The noteworthy feature of the strontium aluminate structure is a puckered six-membered AlO_4 tetrahedral ring, with the average bridging Al—O bond length, 1.768 (8) Å, slightly greater than the average non-bridging Al—O bond length, 1.746 (5) Å. $Sr_3Al_2(O_4D_4)_3$, $M_r = 532.98$, cubic, $Ia3d$, $a = 13.0319\ (1)$ Å, $V = 2213.2\ (2)$ Å^3, $Z = 8$, $D_x = 3.128$ g cm^{-3}, $\lambda = 1.400$ Å, $\mu R = 0.012$, $T = 295$ K, $R_{exp} = 0.0316$, $R_{wp} = 0.0464$ for 2400 step intensities, $R_{Bragg} = 0.0148$ for 224 reflections. $Sr_3Al_2(O_4D_4)_3$ has the hydrogarnet structure, which in contrast to the silicate garnets, has the D_4O_4 unit in place of the SiO_4 unit. The O—D distance is 0.914 (4) Å, and the refined D content of the H position is 90%. Both the Sr hydrogarnet and the aluminate are isostructural with the Ca analogs. The enhanced reactivity of $Sr_3Al_2O_6$ to form the hydrogarnet as compared to that of $Ca_3Al_2O_6$ is ascribed to the increased cell size and strain caused by the substitution of the larger sized Sr for Ca.

Introduction. The conversion of $Ca_3Al_2O_6$ to the hydrogarnet $Ca_3Al_2(O_4H_4)_3$ is one of the principal hydration reactions in the setting of Portland cements. The density decrease for this reaction is 16% for the Ca analogs and 24% for the Sr analogs. A comparison between the Sr and Ca analogs is being made to elucidate the reactivity of the aluminate and the stability of the (O_4H_4) unit. In addition, structural systematics and Al—O bond length and Al—O—Al angle variations among the tetrahedral aluminates are being examined. The crystal structures of the Ca analogs have been determined and studied extensively (Mondal & Jeffery, 1975; Lager, Armbruster & Faber, 1987). The structure of Sr hydrogarnet has been refined only from single-crystal X-ray data (Nevskii, Ivanov-Emin, Nevskaya, Kaziev & Belov, 1982) whereas that of the $Sr_3Al_2O_6$ has not been reported.

Experimental. The strontium aluminate was prepared by the solid-state reaction of high-purity Al_2O_3 and $SrCO_3$ at 1573 K. The hydrogarnet was prepared by adding D_2O to the finely powdered strontium aluminate. The ensuing exothermic hydration reaction proceeds at room temperature, but nearly complete reaction is achieved only by drying the wet powder under a heat lamp. By this method the sample temperature does not exceed 373 K.

The neutron diffraction data were collected on the newly completed HB-4 high-resolution powder diffractometer at the HFIR, ORNL. This instrument has a Ge(115) monochromator which, when $2\theta = 80°$, selects an incident neutron beam of 1.3996 Å. Soller slit collimators of 12′ and 20′ are positioned before and after the monochromator crystal, respectively. An array of 32 equally spaced (2.7°) ^{3}He detectors, each with a 6′ mylar foil collimator, can be step-scanned over a range up to 40° for scattering angles between 11 and 135° in 2θ. The hydrogarnet was placed in a vanadium can (1 × 5 cm) and the $Sr_3Al_2O_6$ was pressed into a 4 × 1 cm rod and used without a cannister. For both samples the data were collected at 295 K over the range 11 to 135° in 2θ in steps of 0.05°. For each step, diffracted beams were accumulated until an incident-beam monitor registered a preset number of counts. For these data collections, the detector array scanned the largest 2θ range allowable, ~40°, which has the effect of overlapping up to 15 detectors for steps in the middle of the pattern. Overlapping detectors for a given step

0108-2701/92/030414-06$03.00

helps to average the counting efficiency and the 2θ zero-point shift for each detector.

The least-squares structure refinements were made with the computer program *LHPM*1 (Hill & Howard, 1986), an extensively modified version of *DBW*3.2 (Wiles & Young, 1981), which uses a full-profile Rietveld analysis (Rietveld, 1969). The Voigt peak-shape function was employed, where the width of the Gaussian component varies as FWHM (Gaussian) $= (U\tan^2\theta + V\tan\theta + W)^{1/2}$ (Caglioti, Paoletti & Ricci, 1958) and the width of the Lorentzian component varies as FWHM(Lorentzian) = $K\sec\theta$ (the Scherrer equation). The background was defined by a fourth-order polynomial in $2\theta^n$, and was refined simultaneously with the other profile and structural parameters. The other refineable profile parameters were the 2θ zero-point, Voigt profile half-width parameters (U, V, W and K) calculated for five half-widths on either side of the peak position, and a peak asymmetry parameter (Howard, 1982) for all reflections. The coherent scattering lengths used were Sr 7.02, Al 3.449, O 5.805, D 6.672 and H 3.741 fm (Koester, Rauch, Herkens & Schroeder, 1981; Sears, 1986). No absorption correction was applied. The function minimized in the least-squares procedure was $\sum w_i(Y_{io} - Y_{ic})^2$, where Y_{io} and Y_{ic} are observed and calculated intensities at each step i in the pattern. The weight w_i assigned to each step intensity is the reciprocal of the variance σ_i^2 at the ith step and was evaluated by $w_i = 1/\sigma_i^2 \simeq n/Y_{io}$ where n is the number of detectors contributing to the average step intensity. The following agreement factors were calculated: $R_p = \sum|Y_{io} - Y_{ic}|/\sum Y_{io}$, $R_{wp} = [\sum w_i(Y_{io} - Y_{ic})^2/\sum w_i Y_{io}^2]^{1/2}$, $R_{\rm exp} = [(N-P)/\sum w_i Y_{io}^2]^{1/2}$, $R_{\rm Bragg} = \sum|I_{ko} - I_{kc}|/\sum I_{ko}$, goodness of fit $= \sum w_i(Y_{io} - Y_{ic})^2/(N-P)$, where N and P are the number of observations and adjustable parameters, respectively.

Starting values for the structural parameters for the refinements were obtained from the structure data of the Ca analogs, $Ca_3Al_2O_6$ (Mondal & Jeffery, 1975) and $Ca_3Al_2(O_4H_4)_3$ (Lager *et al.*, 1987), and peak-shape parameters were assigned based on a previous refinement of a NIST corundum (Al_2O_3) standard. The refinement strategy used as follows: (1) refine the background parameters, 2θ zero-point and scale factor, (2) include the unit cell, peak shape and half-width parameters, (3) include positional parameters, (4) include any site occupancies and (5) include isotropic/anisotropic thermal parameters allowing all adjustable parameters to vary. Preferred orientation was not observed. Refinements were continued until the parameter shifts in the last cycle were less than 10% of their associated e.s.d.'s.

Discussion. Both the Sr hydrogarnet and the aluminate are isostructural with the Ca analogs. $Sr_3Al_2O_6$. There are 14 atoms in the asymmetric unit. The structure was refined to $R_p = 0.0367$, $R_{wp} = 0.0447$, $R_{\rm exp} = 0.0295$, $R_{\rm Bragg} = 0.0168$ and g.o.f. = 0.0230 using 48 structural parameters (with isotropic temperature factors) and 11 profile and background parameters. A summary of the refined structural parameters is given in Table 1, and the corresponding observed, calculated and difference neutron powder diffraction profiles are presented in Fig 1.* The noteworthy feature of the strontium aluminate structure is a puckered six-membered AlO_4 tetrahedral ring, with the average bridging Al—O bond length, 1.768 (8) Å, slightly greater than the average non-bridging Al—O bond length, 1.746 (5) Å (Table 2). In the unit cell (Fig. 2), eight such separate Al_6O_{18} rings surround each of eight vacant sites, and account for all 48 Al and 144 O atoms. Consequently, the O···O separations given in Table 2 for the AlO_4 tetrahedra also apply to the SrO_n polyhedra. The Sr atoms cross-link the aluminate rings and occupy 56 body-centering positions of 64 pseudo-cells ($a' = a/4$). The eight vacant pseudo-cells are situated at $\frac{1}{8}\ \frac{1}{8}\ \frac{1}{8}$ and its symmetry-related positions. The remaining 16 Sr atoms and the 48 Al atoms occupy the corners of the pseudo-cells.

As noted by Mondal & Jeffery (1975) for $Ca_3Al_2O_6$, the presence of short Ca—O bonds and distorted CaO_n polyhedra indicates some amount of strain in the structure, and that this stored energy will be available to assist the break up of the structure in hydration reactions. The same can be said for $Sr_3Al_2O_6$. Moreover, a bond-strength sum analysis, using the bond-strength curves of Brown & Altermatt (1985), for both $Ca_3Al_2O_6$ and $Sr_3Al_2O_6$ provides further support for these ideas. The bond-strength sums for $Sr_3Al_2O_6$ and $Ca_3Al_2O_6$ (given in parentheses) are Al(1) 3.01 (3.05), Al(2) 3.00 (3.03), X(1) 2.28 (2.22), X(2) 2.16 (1.92), X(3) 2.25 (2.10), X(4) 1.53 (1.47), X(5) 1.63 (1.73), X(6) 1.88 (1.93), O(1) 2.01 (2.07), O(2) 2.03 (2.11), O(3) 1.89 (1.87), O(4) 1.83 (1.85), O(5) 1.81 (1.77) and O(6) 1.95 (1.95). The bond-strength sums to the Al, X(2), Ca(3), Ca(6), O(1), O(2), O(3) and O(6) sites are near the ideal values; X(4), X(5), Sr(6), O(3), O(4) and O(5) are significantly underbonded; X(1) and Sr(3) are significantly overbonded. Note that the bond strengths of Sr(1), Sr(2) and Sr(3) are increased relative to Ca(1), Ca(2) and Ca(3). For X(5) and X(6) additional weak bonds to distant O atoms might be included in their coordination spheres; however, the bond-strength sums are improved only slightly. For

* The list of step-scan diffraction data have been deposited with the British Library Document Supply Centre as Supplementary Publication No. SUP 54593 (5 pp.). Copies may be obtained through The Technical Editor, International Union of Crystallography, 5 Abbey Square, Chester CH1 2HU, England. [CIF reference: ST0526]

Table 1. *Fractional atomic coordinates and isotropic thermal parameters for* $Sr_3Al_2O_6$

	x	*y*	*z*	B(Å^2)
Sr(1)	0	0	0	0.5 (1)
Sr(2)	0.5	0	0	0.6 (1)
Sr(3)	0.2519 (1)	0.2519 (1)	0.2519 (1)	0.1 (1)
Sr(4)	0.3759 (2)	0.3759 (2)	0.3759 (2)	0.47 (6)
Sr(5)	0.1343 (2)	0.3750 (2)	0.1319 (2)	0.71 (3)
Sr(6)	0.3799 (2)	0.3855 (1)	0.1247 (1)	0.39 (4)
Al(1)	0.2519 (2)	0.0168 (4)	0.0193 (4)	0.22 (8)
Al(2)	0.2381 (4)	0.2345 (4)	0.0041 (3)	0.35 (9)
O(1)	0.2622 (2)	0.1257 (4)	0.0028 (2)	0.63 (5)
O(2)	0.4928 (2)	0.1295 (3)	0.2437 (2)	0.59 (6)
O(3)	0.2704 (2)	0.2769 (2)	0.1002 (2)	0.70 (5)
O(4)	0.2352 (2)	0.4063 (2)	0.2800 (2)	0.48 (6)
O(5)	0.3460 (2)	−0.0256 (2)	−0.0194 (2)	0.77 (7)
O(6)	0.1539 (2)	−0.0176 (2)	−0.0168 (2)	0.68 (6)

Table 2. *Comparison of interatomic distances* (Å) *and selected angles* (°) *for* $Ca_3Al_2O_6$ *and* $Sr_3Al_2O_6$

		$Ca_3Al_2O_6$*	$Sr_3Al_2O_6$
AlO_4 tetrahedra			
Al(1)—O(1)	br†	1.741 (3)	1.754 (8)
Al(1)—O(2^{viii})	br	1.768 (4)	1.789 (7)
Al(1)—O(5)	nbr	1.766 (3)	1.743 (5)
Al(1)—O(6)	nbr	1.729 (3)	1.748 (5)
Mean		1.751	1.758
O(1)—Al(1)—O(2^{viii})		109.9 (1)	110.5 (3)
O(1)—Al(1)—O(5)		102.9 (1)	104.2 (2)
O(1)—Al(1)—O(6)		111.6 (1)	110.0 (3)
O(2^{viii})—Al(1)—O(5)		103.8 (1)	103.1 (2)
O(2^{viii})—Al(1)—O(6)		105.8 (1)	106.7 (3)
O(5)—Al(1)—O(6)		122.1 (1)	121.6 (3)
Mean		109.3	109.3
O(1)···O(2^{viii})		2.874 (4)	2.912 (6)
O(1)···O(5)		2.743 (4)	2.764 (6)
O(1)···O(6)		2.870 (4)	2.864 (6)
O(2^{viii})···O(5)		2.782 (4)	2.771 (2)
O(2^{viii})···O(6)		2.789 (4)	2.836 (5)
O(5)···O(6)		3.058 (4)	3.048 (4)
Mean		2.853	2.865
Al(2)—O(1)	br	1.749 (3)	1.767 (8)
Al(2)—O(2^{xii})	br	1.764 (3)	1.765 (7)
Al(2)—O(3)	nbr	1.748 (3)	1.742 (4)
Al(2)—O(4^{ix})	nbr	1.757 (3)	1.754 (5)
Mean		1.755	1.757
O(1)—Al(2)—O(2^{xii})		113.5 (1)	113.6 (3)
O(1)—Al(2)—O(3)		108.8 (1)	108.8 (4)
O(1)—Al(2)—O(4^{ix})		100.6 (1)	100.0 (3)
O(2^{xii})—Al(2)—O(3)		107.3 (1)	107.4 (3)
O(2^{xii})—Al(2)—O(4^{ix})		102.4 (1)	103.0 (3)
O(3)—Al(2)—O(4^{ix})		124.0 (1)	123.7 (3)
Mean		109.4	109.4
O(1)···O(2^{xii})		2.937 (4)	2.956 (6)
O(1)···O(3)		2.842 (4)	2.854 (2)
O(1)···O(4)		2.696 (4)	2.699 (6)
O(2^{xii})···O(3)		2.830 (4)	2.827 (5)
O(2^{xii})···O(4^{ix})		2.745 (4)	2.755 (5)
O(3)···O(4^{ix})		3.095 (4)	3.084 (4)
Mean		2.858	2.862
Al(1)—O(1)—Al(2)		150.3 (1)	159.9 (3)
Al(1)—O(2)—Al(2)		154.3 (1)	157.3 (2)
XO_n polyhedra			
X(1)—O(6) × 6		2.338 (3)	2.470 (3)
X(2)—O(5) × 6		2.391 (3)	2.494 (3)
X(3)—O(3) × 3		2.351 (3)	2.455 (3)
X(3)—O(4) × 3		2.357 (3)	2.502 (3)
Mean		2.354	2.478
X(4)—O(1^{vi}) × 3		2.543 (3)	2.701 (4)
X(4)—O(4) × 3		2.526 (3)	2.742 (4)
X(4)—O(5^{vi}) × 3		3.012 (3)	2.935 (4)
Mean		2.693	2.794
X(5)—O(1^{i})		2.471 (3)	2.748 (4)
X(5)—O(2^{i})		2.401 (3)	2.549 (4)
X(5)—O(2^{xii})		2.958 (3)	2.900 (4)
X(5)—O(3)		2.429 (3)	2.707 (4)
X(5)—O(3^{i})		2.969 (3)	2.885 (4)
X(5)—O(4)		2.947 (3)	2.884 (4)
X(5)—O(5^{v})		2.569 (3)	2.887 (4)
X(5)—O(5^{iv})		2.258 (3)	2.428 (4)
Mean		2.625	2.748
X(6)—O(1^{xi})		3.075 (3)	2.867 (2)
X(6)—O(2^{i})		2.462 (3)	2.750 (4)
X(6)—O(3)		2.320 (3)	2.475 (4)
X(6)—O(4^{ii})		2.266 (3)	2.458 (3)
X(6)—O(6^{v})		2.781 (3)	2.771 (3)
X(6)—O(6^{iii})		2.294 (4)	2.440 (4)
X(6)—O(6^{xi})		2.477 (3)	2.716 (4)
Mean		2.525	2.639

* $Ca_3Al_2O_6$ data and symmetry-equivalent atom notation from Mondal & Jeffrey (1975).

† br = bridging and nbr = non-bridging with respect to the tetrahedral aluminate anion.

the other underbonded cation sites no additional O atoms in their coordination spheres are possible. The bond-strength sum analysis identifies the grossly underbonded sites as possible sites of attack by water.

The hydrogarnet forms more readily from $Sr_3Al_2O_6$ than from $Ca_3Al_2O_6$. For the latter, immediately after contact with water the hydration product is $2CaO.Al_2O_3.H_2O$ and at 293 K and above it gradually converts to the hydrogarnet (Mondal & Jeffery, 1975). Complete conversion of $Ca_3Al_2O_6$ to the hydrogarnet requires elevated T and P. For example, Lager *et al.* (1987) used $T = 473$ K and $P(H_2O) = 200$ bars (1 bar = 10^5Pa) for a period of eight days. In contrast, $Sr_3Al_2O_6$ converts to the hydrogarnet at temperatures just above 293 K and at 1 bar, in just a few minutes. Two reasons are suggested for the increased reactivity of $Sr_3Al_2O_6$ relative to $Ca_3Al_2O_6$. First is the increased cell size. The hole at $\frac{1}{8}\ \frac{1}{8}\ \frac{1}{8}$ surrounded by the Al_6O_{18} ring has a larger spherical radius, 1.53 as compared to 1.47 Å for $Ca_3Al_2O_6$ (Mondal & Jeffery, 1975). Indeed, these cavities are connected in the [111] directions to form channels, in which Sr atoms reside, and are also undoubtedly conduits for water. Secondly, the enhanced bond strengths at the $X(1)$, $X(2)$ and $X(3)$ sites indicate a greater amount of strain in $Sr_3Al_2O_6$.

$Sr_3Al_2(O_4D_4)_3$. There are four atoms in the asymmetric unit. The structure was refined to $R_p = 0.0367$, $R_{wp} = 0.0465$, $R_{exp} = 0.0316$, $R_{Bragg} = 0.0149$ and g.o.f. = 0.0216 using 26 structural parameters (with

anisotropic temperature factors) and 11 profile and background parameters. A summary of the refined structural parameters is given in Table 3, and the corresponding observed, calculated and difference neutron powder diffraction profiles are presented in Fig. 3. $Sr_3Al_2(O_4D_4)_3$ has the hydrogarnet structure, which in contrast to the silicate garnets, has O_4D_4 in place of the SiO_4 unit.

The general chemical formula of the hydrogarnet can be represented as $^{[8]}X^{[6]}Y(^{[4]}SiO_4)_{3-x}(O_4H_4)_x$, where the superscripts in brackets refer to the O coordination of the three different types of cations in the structure. The O coordination of the X site defines a triangular dodecahedron (distorted cube) that shares two edges with tetrahedra, four with octahedra (Y site) and four with dodecahedra. The hydrogarnet structure is uniquely defined by the fractional coordinates (xyz) of the O and D atoms

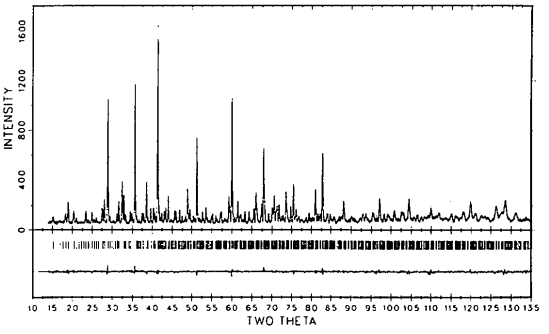

Fig. 1. Observed, calculated and difference neutron powder diffraction profiles for $Sr_3Al_2O_6$. The observed data are indicated by dots and the calculated profile is the continuous solid line in the same field. The short vertical lines below the profiles mark the positions of all possible Bragg reflections, and the bottom curve is the difference between the observed and calculated intensity (plotted using the same vertical scale as the observed and calculated profiles).

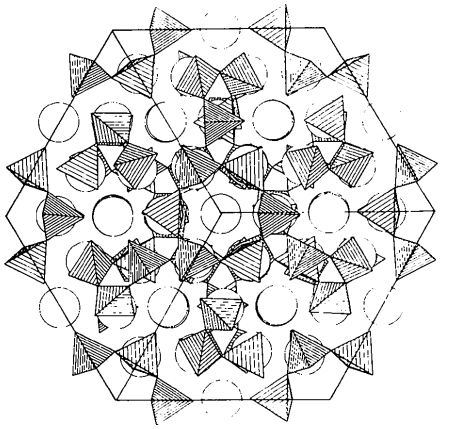

Fig. 2. *STRUPLO* projection (Fischer, 1985) of the contents of one unit cell (outlined) of $Sr_3Al_2O_6$ viewed along [111]. The shaded tetrahedra represent AlO_4 units and the circles Sr atoms.

Table 3. *Fractional atomic coordinates, anisotropic thermal parameters* ($Å^2 \times 10^4$) *and equivalent isotropic thermal parameters* ($Å^2$) *for* $Sr_3Al_2(O_4D_4)_3$

The temperature factor in the expression for the structure factor is defined by $T = \exp[-(\beta_{11}h^2 + \beta_{22}k^2 + \beta_{33}l^2 + 2\beta_{12}hk + 2\beta_{13}hl + 2\beta_{23}kl)]$ and $\beta_{ij} = 2\pi^2 U_{ij}a^*_i a^*_j$. $B_{eq} = (4/3)\sum_i\sum_j \beta_{ij}\mathbf{a}_i\cdot\mathbf{a}_j$.

	x	y	z
Sr	0.125	0	0.25
Al	0	0	0
O	0.0284 (2)	0.0495 (1)	0.6351 (1)
D/H*	0.1547 (3)	0.0961 (2)	0.7895 (2)

	U_{11}	U_{22}	U_{33}	U_{12}	U_{13}	U_{23}	B_{eq}
Sr	137 (17)	52 (9)	52	0	0	0 (4)	0.64
Al	60 (9)	60	60	8 (8)	8	8	0.48
O	60 (9)	146 (9)	112 (9)	8 (4)	−8 (4)	−4 (4)	0.84
D/H	353 (17)	422 (17)	826 (26)	−69 (4)	−60 (8)	95 (8)	4.21

* The refined D content of the H position is 90%.

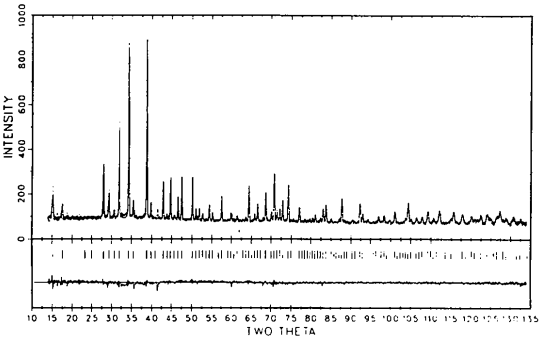

Fig. 3. Observed, calculated, and difference neutron powder diffraction profiles for $Sr_3Al_2(O_4D_4)_3$. The description of the profiles is the same as Fig. 1.

and the unit-cell parameter. The cations occupy special positions that are fixed by symmetry (Table 3). The reader is referred to Novak & Gibbs (1971) for a complete description of the garnet structure.

The refined O position in $Sr_3Al_2(O_4D_4)_3$ is within one e.s.d. of that determined by single-crystal X-ray diffraction methods (Nevskii *et al.*, 1982). As one might expect, the X-ray H position reported by Nevskii *et al.* (1982) [0.162 (4), 0.105 (4), 0.790 (4)] differs considerably from the D position refined from the neutron powder data collected in this study. The O—D distance in $Sr_3Al_2(O_4D_4)_3$ is within two e.s.d.'s of the corresponding distance in the Ca analog (Table 4). However, both of these distances are short in comparison to other O—D distances determined by neutron diffraction methods (mean value = 0.969 (1) Å; Ceccarelli, Jeffrey & Taylor, 1981). Two reasons can be cited for the shorter-than-average bond length. First, O—D distances in both Ca and Sr hydrogarnet have not been corrected for the librational motion of the D atom. In view of the large mean-square displacement of D perpendicular to the O—D bond (Fig. 4), such a correction would be expected to increase the length of the O—D bond.

Table 4. *Comparison of interatomic distances* (Å) *and selected angles* (°) *for* $Ca_3Al_2(O_4D_4)_3$ *and* $Sr_3Al_2(O_4D_4)_3$

Atom-label nomenclature is after Novak & Gibbs (1971).

	$Ca_3Al_2(O_4D_4)_3$†	$Sr_3Al_2(O_4D_4)_3$
Tetrahedron		
d—O‡ × 4	1.950 (2)	2.059 (1)
O(1)—*d*—O(2) × 2	103.3 (2)	104.6 (1)
O(1)—*d*—O(3) × 4	112.7 (2)	111.9 (1)
Mean	109.5	109.5
O(1)···O(2) × 2	3.058 (2)	3.260 (1)
O(1)···O(3) × 4	3.245 (2)	3.414 (2)
Mean	3.183	3.337
Octahedron		
Al—O × 6	1.916 (2)	1.911 (1)
O(1)—Al—O(4) × 6	85.6 (2)	86.1 (1)
O(1)—Al—O(5) × 6	94.4 (2)	93.8 (1)
Mean	90.0	89.9
O(1)···O(4) × 6	2.604 (2)	2.610 (3)
O(1)···O(5) × 6	2.811 (2)	2.792 (2)
Mean	2.707	2.701
Dodecahedron		
X(1)—O(4) × 4	2.464 (2)	2.579 (2)
X(2)—O(4) × 4	2.521 (2)	2.642 (1)
Mean	2.493	2.610
O(1)—*X*—O(2) × 2	76.7 (1)	78.4 (1)
O(1)—*X*—O(4) × 4	62.9 (1)	59.9 (1)
O(1)—*X*—O(7) × 4	97.1 (1)	97.3 (1)
O(4)—*X*—O(6) × 4	76.0 (1)	78.1 (1)
O(4)—*X*—O(7) × 2	73.9 (1)	74.0 (1)
O(7)—*X*—O(8) × 2	106.8 (1)	108.0 (1)
Mean	81.0	81.2
O(1)···O(2) × 2	3.058 (2)	3.260 (1)
O(1)···O(4) × 4	2.604 (2)	2.610 (3)
O(1)···O(7) × 4	3.736 (2)	3.920 (2)
O(4)···O(6) × 4	3.071 (2)	3.293 (3)
O(4)···O(7) × 2	3.030 (2)	3.182 (2)
O(7)···O(8) × 2	4.048 (2)	4.175 (5)
Mean	3.218	3.363
(O_4D_4) tetrahedral environment		
About O(1)—O(3)		
O—D × 4	0.906 (2)	0.914 (4)
O···D	2.567 (2)	2.697 (3)
	2.497 (2)	2.669 (3)
D—D	1.956 (2)	2.068 (4)
O···D—O	132.1 (1)	135.8 (2)
	140.1 (1)	139.0 (2)
O—O···D	12.0 (1)	10.7 (1)
	10.3 (1)	10.1 (1)
O—O—D	36.0 (1)	33.4 (1)
	29.6 (1)	30.9 (1)
About O(1)—O(2)		
O···D	2.959 (2)	3.109 (3)
D—D	2.599 (2)	2.708 (5)
O···D—O	87.5 (1)	91.3 (1)
O—O···D	17.2 (1)	16.3 (1)
O—O—D	75.3 (1)	72.5 (1)
Other distances involving deuterium		
d—D	1.343 (2)	1.408 (2)
Al—D	2.425 (2)	2.414 (3)
X(1)—D	3.094 (2)	3.174 (3)
X(2)—D	2.851 (2)	3.034 (2)

† Data from Lager *et al.* (1987).

‡ *d* is the Wyckoff notation for the position with point symmetry $\bar{4}$ in space group *Ia3d* (occupied by Si in silicate garnets).

Secondly, the mean-square displacement amplitudes of D in $Ca_3Al_2(O_4D_4)_3$ (Lager *et al.*, 1987) show only minor changes on cooling from 300 to 100 K, which suggests the possibility of static positional disorder of the D atom in hydrogarnet structures and an apparent shortening of the O—D bond length.

The D atoms in $Sr_3Al_2(O_4D_4)_3$ are located slightly above the faces of the O tetrahedron in approximately the same orientation as observed for the Ca analog (Table 4). The closest O neighbor to D is located along the edge O(1)—O(3), 2.669 (3) Å from D (Table 4). Since this distance is about equal to the sum of the van der Waals radii for H and O (2.69 Å) (Downs & Ross, 1987, and references therein), a 'free' non-hydrogen-bonded OH group exists in Sr hydrogarnet. The (O_4D_4) tetrahedron in the Ca analog is smaller and the above O···D distance [2.497 (2) Å] is correspondingly shorter, indicating a very weak O—H···O interaction.

$Sr_3Al_2(O_4H_4)_3$, $Sr_3Fe_2(O_4H_4)_3$ (Nevskii *et al.*, 1982) and $Ca_3Al_2(O_4H_4)_3$ represent the only Si-free hydrogarnets that have been synthesized to date. There exists a complete solid-solution series ($0 \le x \le 1$) between $Ca_3Al_2(O_4H_4)_3$ (katoite) and $Ca_3Al_2(SiO_4)_3$ (grossular). The extent of solid solutions beween the Sr analogs is unknown; however, Novak & Gibbs (1971) have predicted that substitution of the large Sr^{2+} cation in the *X* site will introduce a number of destabilizing features in the anhydrous garnet [$Sr_3Al_2(SiO_4)_3$] structure. To the authors' knowledge, this garnet has not been synthesized. No appreciable $(O_4H_4) \leftrightarrow (SiO_4)$ substitution (< 0.25 wt% OH) has been observed for pyrope [$Mg_3Al_2(SiO_4)_3$] and other pyralspite garnets (Aines & Rossman, 1984). Naturally occurring andradites [$Ca_3(Fe,Ti)_2(SiO_4)_3$] have been reported with OH contents to ≃ 6 wt% OH ($x = 0.15$) (Basso, Cimmino & Messiga, 1984*a*, *b*; Lager, Armbruster, Rotella & Rossman, 1989).

A bond-strength sum analysis for the *X* site provides some useful insights into the question of why the $(O_4H_4) \leftrightarrow (SiO_4)$ substitution is more common

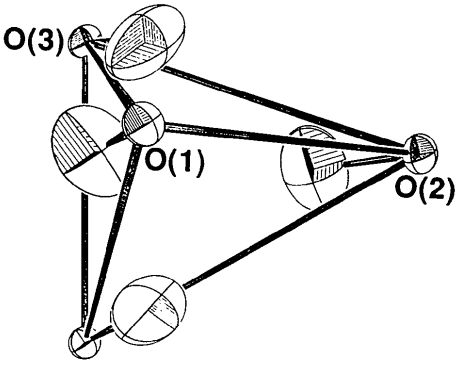

Fig. 4. *ORTEP*II plot (Johnson, 1976) of the atomic environment about the $\bar{4}$ site in $Sr_3Al_2(O_4D_4)_3$ showing the O tetrahedron with associated D atoms.

in particular garnet compositions rather than others. In what follows, the bond-strength sums for the X cation are related to the occupations of the X and Y sites and x as defined by the hydrogarnet formula: 2.12 (X = Sr, Y = Al, x = 3); 3.07 (X = Sr, Y = Al, x = 0); 1.93 (X = Ca, Y = Al, x = 3); 2.52 (X = Ca, Y = Al, x = 0); 2.31 (X = Ca, Y = Fe, x = 0); 1.72 (X = Mg, Y = Al, x = 0). For $Sr_3Al_2(SiO_4)_3$ (X = Sr, Y = Al, x = 0) bond-strength sums were calculated from the Sr—O distances predicted by Novak & Gibbs (1971). The bond-strength sums to Ca in grossular and andradite indicate a significant amount of overbonding, *i.e.* Ca is too large for the dodecahedral cavity based on a comparison of the mean Ca—O distances (2.405 and 2.433 Å for grossular and andradite, respectively) and the sum of the ionic radii for $^{[8]}$Ca and $^{[4]}$O (2.50 Å) (Shannon, 1976). Underbonding of the X site in pyrope also reflects a size misfit, but in this case, Mg is too small for the cavity. As the substitution $(O_4H_4) \leftrightarrow (SiO_4)$ causes an expansion of the dodecahedron (Lager *et al.*, 1989), overbonded sites will be stabilized and underbonded sites destabilized as the OH content increases (Zabinski, 1966). This line of reasoning is consistent with experimental data for grossular, andradite and pyrope (see above). The extreme overbonding at the X site in $Sr_3Al_2(SiO_4)_3$ may be the reason that this garnet has not been synthesized. Based on these simple arguments, a limited $(O_4H_4) \leftrightarrow (SiO_4)$ substitution should exist for Sr garnets; however, the stability field will be displaced, relative to the Ca analogs, toward the hydrogarnet end member.

This research was supported by the Division of Materials Sciences, US Department of Energy, under contract No. DE-AC05-84OR21400 with Martin Marietta Energy Systems. GAL acknowledges support of this research by the National Science Foundation (Experimental and Theoretical Geochemistry) through grant EAR-8719848.

References

AINES, R. D. & ROSSMAN, G. R. (1984). *Am. Mineral.* **69**, 1116–1126.
BASSO, R., CIMMINO, F. & MESSIGA, B. (1984*a*). *Neues Jahrb. Mineral. Abh.* **148**, 248–258.
BASSO, R., CIMMINO, F. & MESSIGA, B. (1984*b*). *Neues Jahrb. Mineral. Abh.* **150**, 247–258.
BROWN, I. D. & ALTERMATT, D. (1985). *Acta Cryst.* B**41**, 244–247.
CAGLIOTI, G., PAOLETTI, A. & RICCI, F. P. (1958). *Nucl. Instrum.* **3**, 223–228.
CECCARELLI, C., JEFFREY, G. A. & TAYLOR, R. (1981). *J. Mol. Struct.* **70**, 255–271.
DOWNS, J. W. & ROSS, F. K. (1987). *Am. Mineral.* **72**, 979–983.
FISCHER, R. X. (1985). *J. Appl. Cryst.* **18**, 258–262.
HILL, R. J. & HOWARD, C. J. (1986). *A Computer Program for Rietveld Analysis of Fixed Wavelength X-ray and Neutron Powder Diffraction Patterns.* Report No. M112. Australian Nuclear Science and Technology Organization, Lucas Heights Research Laboratories, PMB, Sutherland, New South Wales, Australia.
HOWARD, C. J. (1982). *J. Appl. Cryst.* **15**, 615–620.
JOHNSON, C. K. (1976). *ORTEP*II. Fortran thermal ellipsoid plot program for crystal structure illustrations, p. 125. US Department of Commerce, National Technical Information Service, Springfield, Virginia, USA.
KOESTER, L., RAUCH, H., HERKENS, M. & SCHROEDER, K. (1981). Kerforschungsanlage Julich, report 1755.
LAGER, G. A., ARMBRUSTER, T. & FABER, J. (1987). *Am. Mineral.* **72**, 756–765.
LAGER, G. A., ARMBRUSTER, T., ROTELLA, F. J. & ROSSMAN, G. R. (1989). *Am. Mineral.* **74**, 840–851.
MONDAL, P. & JEFFERY, J. W. (1975). *Acta Cryst.* B**31**, 689–697.
NEVSKII, N. N., IVANOV-EMIN, B. N., NEVSKAYA, N. A., KAZIEV, G. Z. & BELOV, N. V. (1982). *Sov. Phys. Dokl.* **27**, 427–428.
NOVAK, G. A. & GIBBS, G. V. (1971). *Am. Mineral.* **56**, 791–825.
RIETVELD, H. M. (1969). *J. Appl. Cryst.* **2**, 65–71.
SEARS, V. F. (1986). *Methods of Experimental Physics*, Vol. 23, Part A, edited by K. SKOLD & D. L. PRICE, pp. 521–550. Orlando: Academic Press.
SHANNON, R. D. (1976). *Acta Cryst.* A**32**, 751–767.
WILES, D. B. & YOUNG, R. A. (1981). *J. Appl. Cryst.* **14**, 149–151.
ZABINSKI, W. (1966). *Pr. Mineral.* **3**, 1–69.

Acta Cryst. (1992). C**48**, 419–424

Structure of Sodium Perbromate Monohydrate

BY ANTHONY C. BLACKBURN, JUDITH C. GALLUCCI, ROGER E. GERKIN* AND WILLIAM J. REPPART†

Department of Chemistry, The Ohio State University, Columbus, Ohio 43210, *USA*

(*Received* 4 *March* 1991; *accepted* 12 *September* 1991)

Abstract. $NaBrO_4.H_2O$, M_r = 184.90, monoclinic, $C2/c$, a = 15.7575 (19), b = 5.7373 (15), c = 11.3390 (19) Å, β = 111.193 (10)°, V = 955.8 (3) Å^3, Z = 8, D_x = 2.570 g cm^{-3}, λ(Mo $K\bar{\alpha}$) = 0.71073 Å, μ = 85.2 cm^{-1}, $F(000)$ = 704, T = 296 K, R = 0.039 for 1137 unique reflections having $I > \sigma_I$. In this structure, there are two inequivalent Na ions, each coordinated by six O atoms. In each of the two types

* Corresponding author.
† Present address: Shell Development Company, Houston, Texas 77001, USA.

0108-2701/92/030419-06$03.00